Available online at www.sciencedirect.com
ScienceDirect
Bioorganic & Medicinal Chemistry Letters 18 (2008) 665–669
Bioorganic & Medicinal Chemistry Letters

Complexation of single strand telomere and telomerase RNA template polyanions by deoxyribonucleic guanidine (DNG) polycations: Plausible anticancer agents

Xiaohua Zhang and Thomas C. Bruice*

Department of Chemistry and Biochemistry, University of California, Santa Barbara, Santa Barbara, CA 93106, USA

Received 16 October 2007; accepted 16 November 2007
Available online 21 November 2007

Abstract—Cancerous cell immortality is due to relatively high concentrations of telomerase enzyme which maintains telomere sequence during cell division. Deoxyribonucleic guanidine (DNG) is a positively charged DNA analog in which guanidine replaces the phosphordiester linkage of DNA. Mixed sequences of DNG and DNA oligonucleotides are referred to as chimera. Complexation of DNG and chimeric polycations with the complementary negatively charged non-coding telomere single strand d(5′-TTAGGG-3′)$_n$ and the 11-base telomeric RNA template (5′-CUAACCCUAAC-3′) in the active site of telomerase has been studied. Calculated by ensemble sampling simulations in GBMV solvent model, we found that binding of complementary DNG hexamer with telomere is favored over that of DNA-telomere by $\sim 10^6$-fold and binding of chimera hexamer is favored by $\sim 10^4$-fold. Binding of complementary DNG with telomeric RNA is favored by 43 kcal/mol over telomere substrate binding with telomeric RNA.

Telomeres are non-coding DNA repetitive sequences that cap the 3′-end of the chromosome to prevent loss of vital genetic information during cell division.[1] Human telomeric DNA consists of repeats of the sequence d(5′-TTAGGG-3′) on one strand and a complementary sequence on the matching strand (3′-AATCCC-5′). The matching strand is shorter than the repetitive telomere sequence by 150–300 bases.[2,3] The telomere single strand serves as substrate for the telomerase enzyme, which rebuilds the telomere strand lost during cell division. The telomerase enzyme is comprised of a reverse transcriptase protein and a telomeric RNA 11-base template (5′-CUAACCCUAAC-3′).[4] The telomerase synthesis of telomere is regulated by telomere-specific proteins such as protection of telomeres-1 (POT1).[5] A model, provided by Lei et al., demonstrated that in cell division the length of 3′-end overhanging telomere single strand from POT1 is crucial to the synthesis of telomere sequences.[6] Telomerase catalysis is inactive when the overhanging telomere single strand consists of less than six nucleotides (such as TTAGGG), while it is highly active when the single strand contains more than eight nucleotides.

Each time a cell divides, the telomere is shortened in the daughter strand. Continued shortening of the telomere results in decreased cell longevity. Cancer cells contain an abundance of telomerase, which makes them immortal. Two possible approaches to prevent telomere replacement in cancerous cells follow: (a) altering the overhanging telomere single strand so that it is no longer a substrate for the telomerase enzyme; and (b) inhibition of the telomerase enzyme by blocking the telomeric RNA 11-base template.

Telomerase inhibition is a well-known approach to cancer therapeutics.[4] The DNA substrate of telomerase is a polyanion. Drugs invented as inhibitors of enzymes operating on DNA are also generally polyanions. One example is GRN163L (5′-pam-TAGGGTTAGACAA-NH_2-3′), a lipid conjugated 13-mer thiophosphoramidite oligomer (Geron Corporation, California) that is reported to inhibit human telomerase and has clearance by the US FDA to enter human phase I/II of clinical testing against chronic lymphocytic leukeimia and breast cancer.[7]

Abbreviations: DNG, deoxyribonucleic guanidine; GBMV, Generalized Born Molecular Volume.

Keywords: DNA; Nucleic acid analogs; Molecular dynamics.

* Corresponding author. Tel.: +1 805 893 2044; fax: +1 805 893 2229; e-mail: tcbruice@chem.ucsb.edu

0960-894X/$ - see front matter © 2007 Elsevier Ltd. All rights reserved.
doi:10.1016/j.bmcl.2007.11.061

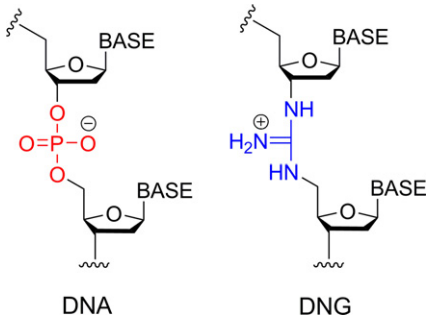

Figure 1. Comparison of DNA and DNG structures.

Since DNA is a polyanion, a polycationic complementary nucleotide sequence to a given DNA target may prove useful. To this end, DNG and RNG compounds were invented. The structure of DNG and RNG differs from that of DNA and RNA (Fig. 1) through replacement of the DNA negatively charged phosphordiester linkages by positively charged guanidinium linkages.[8–10] Polyanion DNA binds to polycation DNG with high affinity and sequence specificity. Moreover, DNG intervenes less with telomere-specific proteins due to the positively charged binding sites of these proteins. Chimeric sequences of DNG and DNA nucleotides have also been introduced.[11]

The CHARMM27 all-atom nucleic acid residue force field was employed in the simulations.[12] The starting structures employed in this study were constructed using the Nucleic Acid Builder (NAB),[13] selecting the B form of DNA as initial conformers. The replacement of phosphodiester linkages with the guanidinium linkage was carried out using the patch command in CHARMM. Langevin dynamics were employed in the integration of the equations of motion with a time step of 1.5 fs. All the trajectories were followed to 6 ns. Binding affinities of DNG/chimera with telomere single strand and telomeric RNA were calculated by ensemble sampling.

Due to the computational cost an implicit solvent model, Generalized Born Molecular Volume (GBMV), was employed in the simulation.[14,15] Generalized Born (GB) model is one of the most popular approaches to approximate the solvent as continuum electrostatics. In GBMV model, a molecular volume correction term has also been introduced to correctly describe the solvent-excluded volume of each pair of atoms to yield better conformational ensembles.[16,17] A benchmark study of DNA simulation using GBMV has been carried out by Chocholousova et al.,[18] which demonstrates that the results of GBMV simulations are in good agreement with either experimental data or explicit solvent simulations. As suggested by professor Feig, the GBMV parameters in this study were set to resemble the water solvent as follows: $\beta = -12$, $S_0 = 0.65$, $C_0 = -0.1$, $C_1 = 0.9$. The definition of GBMV parameters can be found in Lee et al.'s papers.[14,15] The GB radii were taken from the CHARMM force field Lennard–Jones σ values. The hydrophobic contribution to the solvation free energy was obtained based on the solvent accessible surface area (SASA) calculation implemented within the GBMV module. The radius of probe sphere for the SASA calculation was set to 1.4 Å. A dielectric constant of 80.0 was used for the GB continuum solvent model. In order to study the effect of the ionic strength on the binding affinity, two different ionic strengths (μ), 0.12 (physiological condition) and 1.0, were used in the binding affinity calculations.

The helical parameters of dodecamer and hexamer duplexes were calculated by FREEHELIX program.[19] To

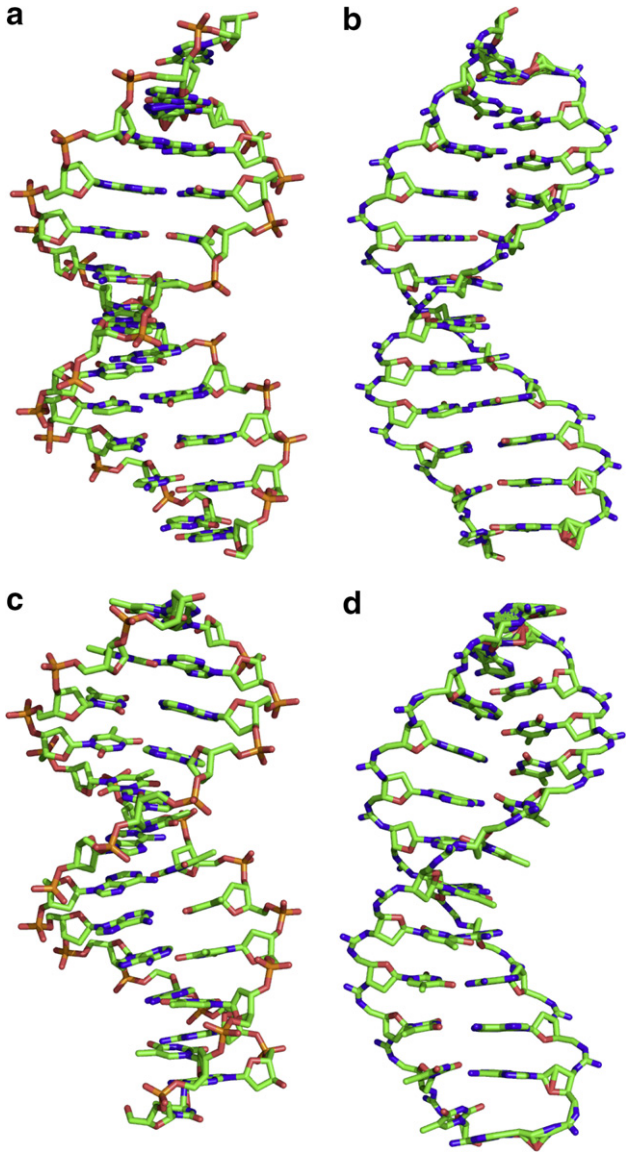

Figure 2. Average structures of (a) $d(Gp)_{12}{\cdot}d(Cp)_{12}$, (b) $d(Gg)_{12}{\cdot}d(Cg)_{12}$, (c) $d(Ap)_{12}{\cdot}d(Tp)_{12}$, and (d) $d(Ag)_{12}{\cdot}d(Tg)_{12}$ duplexes in CPK model. Structures are averaged from 6 ns MD simulations. Only heavy atoms are shown in the figure. Atoms are colored by atom type. Critical helical parameters: rises of helixes are (a) 3.3 ± 0.4, (b) 3.5 ± 0.6, (c) 3.2 ± 0.6, and (d) 3.5 ± 0.7Å; twisted angles are (a) 35.8 ± 3.0°, (b) 28.3 ± 6.3°, (c) 34.0 ± 5.1°, and (d) 29.8 ± 7.2°; helical bendings are (a) 13.1 ± 6.7°, (b) 18.9 ± 9.7°, (c) 15.7 ± 7.9°, and (d) 20.1 ± 9.1°. Major groove width: (a) 16.5 ± 0.8 Å, (b) 20.6 ± 1.1, (c) 17.8 ± 0.7, and (d) 21.3 ± 0.9 Å. Minor groove width: (a) 14.2 ± 0.6 Å, (b) 12.8 ± 0.8, (c) 13.7 ± 0.6, and (d) 12.9 ± 0.8 Å.

reduce the effect of terminal base pairs, only the central base steps and base pairs of each dodecamer/hexamer were evaluated. The major groove width is defined as inter-strand phosphorous atoms (or guanidinium carbons, CG1) $P(i-2)\cdots P'(i+2)$ across the major groove with four base pair separation, while minor groove width is defined as $P'(i-2)\cdots P(i+2)$ across the minor groove separated by three base pairs.

Simulations of structures of $d(Ag)_{12}\cdot d(Tg)_{12}$ and $d(Gg)_{12}\cdot d(Cg)_{12}$ DNG dodecamers were carried out using the GBMV model ('g' denotes guanidinium linkage and 'p' represents phosphate linkage). Results were compared to that of their corresponding DNA dodecamers, $d(Ap)_{12}\cdot d(Tp)_{12}$ and $d(Gp)_{12}\cdot d(Cp)_{12}$ (Fig. 2). In a previous study by Toporowski et al.,[20] simulations of DNG duplexes were performed in explicit TIP3P water. The differences in structure of DNA and DNG duplexes, originating from the sp^2 hybridized guanidinium group and sp^3 phosphate, have been described.[20] These results are consistent with the results of the GC and AT dodecamers obtained from current GBMV simulations. The helix rise of DNG is slightly larger than those of DNA and the twist angle of DNG is smaller

Table 1. The calculated binding affinity of various DNA, chimeras, DNG sequences with telomere and telomeric RNA strand of telomerase enzyme at different ionic concentrations

	Sequence[a]	Binding Affinity (kcal/mol)[b]	
		$\mu_1 = 0.12$ [c]	$\mu_2 = 1.0$
Telomere single Strand			
	5'-TTAGGGTTAGGG-3'		
Hexamer			
DNA	3'-ATCCCA-5'	-45.9	-48.2
Chimera	3'-ATCCCA-5'	-51.5	-51.2
DNG	3'-ATCCCA-5'	-53.3	-52.1
Dodecamer			
DNA	3'-AATCCCAATCCC-5'	-89.5	-93.2
Chi-1	3'-AATCCCAATCCC-5'	-111.5	-111.1
Chi-2	3'-AATCCCAATCCC-5'	-116.7	-116.6
Chi-3	3'-AATCCCAATCCC-5'	-112.4	-111.7
Chi-4	3'-AATCCCAATCCC-5'	-110.9	-110.3
DNG	3'-AATCCCAATCCC-5'	-139.7	-133.4
Telomeric RNA 11-Base Template			
	5'-CUAACCCUAAC-3'		
DNA	3'-GATTGGGATTG-5'	-69.4	-76.8
DNG	3'-GATTGGGATTG-5'	-112.1	-107.3

[a]DNG nucleotides are in red and DNA in black.
[b]Binding affinity is calculated by the equation: $\Delta\Delta G_{binding} = \Delta G_{complex} - \Delta G_{receptor} - \Delta G_{ligand}$.
[c]μ_1 ionic strength at physiological conditions.

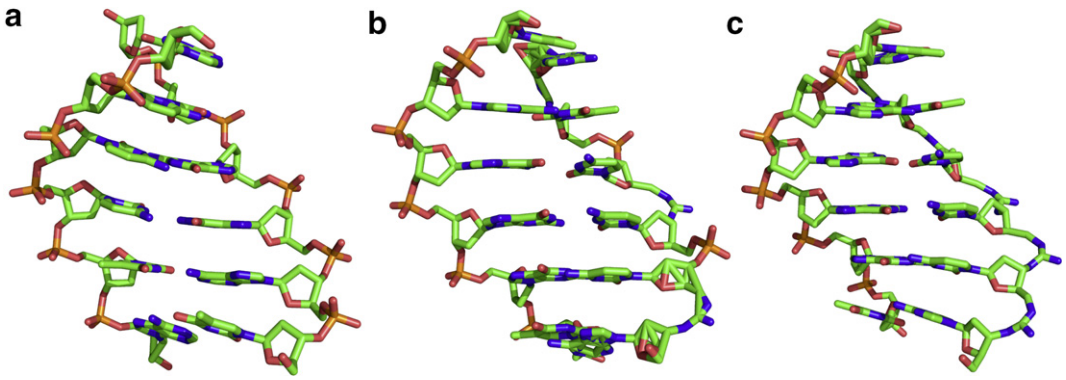

Figure 3. Average structures of (a) DNA-, (b) chimera-, and (c) DNG-bound telomere hexamers from 6 ns MD simulations. Structures are depicted in sticks model. Only heavy atoms are shown in the figure. Atoms are colored by types. Critical helical parameters: Rises of helixes are (a) 3.3 ± 0.5, (b) 3.3 ± 0.4, and (c) 3.4 ± 0.3 Å; twisted angles are: (a) 35.5 ± 4.0°, (b) 35.4 ± 5.9°, and (c) 33.1 ± 4.4°.

than that of DNA. DNG dodecamers also have wider major groove and larger helix bending.

DNG (5′-AgCgCgCgTgA-3′) and chimera (5′-AgCpCgCpTgA-3′) hexamers have been designed to complement telomere segment (5′-TpApGpGpGpT-3′). The MD dynamics structures of DNA, the chimeric, and DNG hexamer complex with telomeres were obtained. The binding energies for different duplexes were calculated (Table 1). At physiological ionic strength ($\mu = 0.12$), the binding free energies of telomere single strand with 5′-TpApGpGpGpT-3′:5′-AgCpCgCpTgA-3′:5′-AgCgCgCgTgA-3′ are −45.9:−51.5:−53.3 kcal/mol, respectively. Thus, binding constant of DNG hexamer with telomere is approximately 10^6-fold greater than that for the DNA hexamer with telomere. Binding constant of chimera hexamer with telomere is approximately 10^4-fold greater than that for the DNA hexamer with telomere.

The critical helical parameters for the DNA, chimera, and DNG hexamer-bound telomere are shown in Figure 3. The rise between nucleotide bases for the chimera-bound telomere strand is the same as that of DNA duplex. The helix rise for the DNG-bound telomere is slightly larger than that of DNA duplex by 0.1 Å, which is due to the stretching of the DNG single strand. The twist angles of DNG-bound telomere are smaller than that of DNA- and chimera-bound telomere by about 2°. This is the result of less twist in the DNG strand.

The Watson–Crick hydrogen bonds between base pairs in DNA, chimera, and DNG hexamer-bound telomere are similar to each other. The base pairs between DNG/chimera and telomere are the same as those in the DNA duplex. The Watson–Crick base pairing is not affected by the replacement of the phosphate linkage with guanidinium linkage. Binding of both DNG and

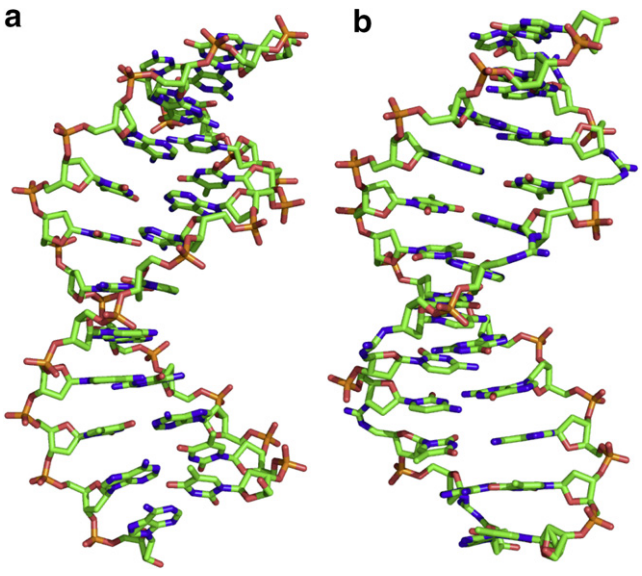

Figure 4. Average structures of (a) DNA and (b) Chi-1 bound telomere dodecamers. Structures are depicted in sticks model. Only heavy atoms are shown in the figure. Atoms are colored by types.

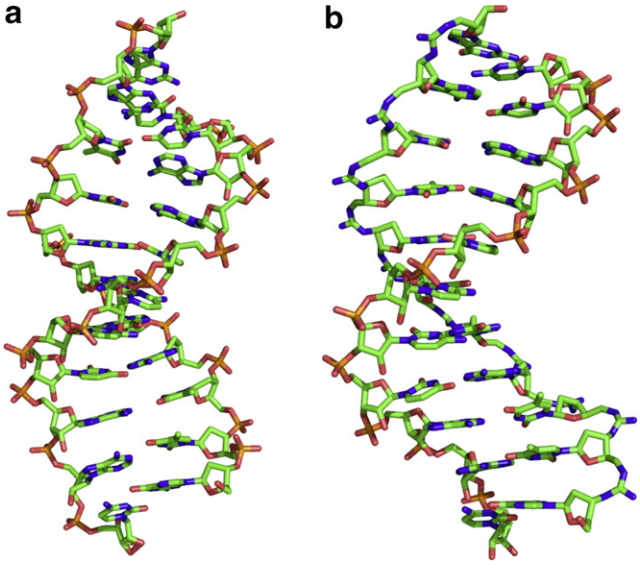

Figure 5. Average structures of (a) DNA and (b) DNG binding with telomeric RNA 11-base template. Structures are depicted in sticks model. Only heavy atoms are shown in the figure. Atoms are colored by types.

chimera with telomere is sequence specific. The telomere sequence was aligned with human genomes by the BLAST[21] program on the NCBI website. No significant similarity is found between telomere sequence and segments of human genome. Thus, the DNG and chimera sequences complementary to the telomere sequence should not interfere with the human genome carrying gene information.

A DNG dodecamer and a series of chimera dodecamers have been studied (Table 1). The geometry of Chi-1 dodecamer-bound telomere resembles closely that of DNA dodecamer-bound telomere. Both of them have similar helical rise, twisted angle, major groove width, and minor groove width (Fig. 4). For the Chi-2, Chi-3, Chi-4, and DNG dodecamers, the helical rise and twisted angle are different. Binding of telomere with DNG is tightest. The nucleotides of Chi-1, Chi-2, Chi-3, and Chi-4 are linked by the same number of guanidinium linkages (Table 1). Binding affinity of various chimeras with telomere ranges from −111 to −117 kcal/mol. The dodecamer ligands are, as expected, more effective in binding with the telomere than the hexamer ligands.

Change of the ionic strength from physiological $\mu = 0.12$–1.0 only slightly affects the binding affinities between the chimera and telomere single strand, where the binding constants differ by less than 1.0 kcal/mol (Table 1). As expected, binding affinities between DNG hexamer/dodecamer and telomere decrease as the ionic concentration increases from $\mu = 0.12$–1.0.

The second approach to telomere regeneration is to inhibit the telomerase enzyme by blocking the telomeric RNA 11-base template. Due to lack of an X-ray structure for telomerase, only the binding between DNG and telomeric RNA 11-base template could be calculated (Fig. 5). The binding affinity of the DNG (3′-GgAgTgTgGgGgGgAgTgTgG-5′) with telomeric RNA is greater than that of corresponding DNA by 43 kcal/mol (Table 1). The binding of DNG with telomeric RNA is so favorable that the interaction between DNG and the telomerase (excluding telomeric RNA) cannot resist DNG and telomeric RNA coming together. It is most possible that DNG is also an ideal ligand to inhibit the telomerase enzyme.

In summary, DNG polynucleotides and DNG/DNA mixed sequences (chimera) bind complementary telomere single strand and telomeric RNA with high sequence specificity. DNG/chimera sequences complementary to the telomere sequence should not interfere with coding sequences because the telomere sequence is not found in coding regions of the human genome. Various DNG and chimera sequences complementary to the telomere single strand and the telomeric RNA 11-base template in the active site of telomerase have been studied. Geometries of the chimeric hexamer- and Chi-1 dodecamer-bound telomere resemble closely their DNA counterparts. Binding of DNG hexamer with telomere is favored over that of DNA by about 10^6-fold. Binding of the chimeric hexamer with the telomere is favored over that of DNA by approximately 10^4-fold. Complementary DNG has great binding affinity with telomeric RNA, which suggests that it could be a promising telomerase inhibitor.

Acknowledgments

We express appreciation to the National Institutes of Health Grant (5R37DK9174-43) and the National Partnership for Advanced Computational Infrastructure for its generous allocation (MCB050064) of computational resources. The authors thank Professor Kevin Plaxco and Professor Charles Brooks for their helpful discussions.

References and notes

1. Blackburn, E. H. *Nature* **1991**, *350*, 569.
2. Makarov, V. L.; Hirose, Y.; Langmore, J. P. *Cell* **1997**, *88*, 657.
3. McElligott, R.; Wellinger, R. J. *EMBO J.* **1997**, *16*, 3705.
4. White, L. K.; Wright, W. E.; Shay, J. W. *Trends Biotechnol.* **2001**, *19*, 114.
5. Lei, M.; Baumann, P.; Cech, T. R. *Biochemistry* **2002**, *41*, 14560.
6. Lei, M.; Zaug, A. J.; Podell, E. R.; Cech, T. R. *J. Biol. Chem.* **2005**, *280*, 20449.
7. Herbert, B. S.; Gellert, G. C.; Hochreiter, A.; Pongracz, K.; Wright, W. E.; Zielinska, D.; Chin, A. C.; Harley, C. B.; Shay, J. W.; Gryaznov, S. M. *Oncogene* **2005**, *24*, 5262.
8. Dempcy, R. O.; Browne, K. A.; Bruice, T. C. *Proc. Natl. Acad. Sci. U.S.A.* **1995**, *92*, 6097.
9. Dempcy, R. O.; Browne, K. A.; Bruice, T. C. *J. Am. Chem. Soc.* **1995**, *117*, 6140.
10. Dempcy, R. O.; Almarsson, O.; Bruice, T. C. *Proc. Natl. Acad. Sci. U.S.A.* **1994**, *91*, 7864.
11. Barawkar, D. A.; Kwok, Y.; Bruice, T. W.; Bruice, T. C. *J. Am. Chem. Soc.* **2000**, *122*, 5244.
12. Foloppe, N.; MacKerell, A. D. *J. Comput. Chem.* **2000**, *21*, 86.
13. Macke, T.; Case, D. A. Modeling Unusual Nucleic Acid Structures. In *Molecular Modeling of Nucleic Acids*; Leontes, N. B., SantaLucia, J., Jr., Eds.; American Chemical Society: Washington, DC, 1998; pp 379–393.
14. Lee, M. S.; Feig, M.; Salsbury, F. R.; Brooks, C. L. *J. Comput. Chem.* **2003**, *24*, 1348.
15. Lee, M. S.; Salsbury, F. R.; Brooks, C. L. *J. Chem. Phys.* **2002**, *116*, 10606.
16. Chen, J. H.; Im, W. P.; Brooks, C. L. *J. Am. Chem. Soc.* **2006**, *128*, 3728.
17. Mongan, J.; Simmerling, C.; McCammon, J. A.; Case, D. A.; Onufriev, A. *J. Chem. Theory Comput.* **2007**, *3*, 156.
18. Chocholousova, J.; Feig, M. *J. Phys. Chem. B* **2006**, *110*, 17240.
19. Dickerson, R. E.; Chiu, T. K. *Biopolymers* **1997**, *44*, 361.
20. Toporowski, J. W.; Reddy, S. Y.; Bruice, T. C. *Bioorg. Med. Chem.* **2005**, *13*, 3691.
21. Altschul, S. F.; Gish, W.; Miller, W.; Myers, E. W.; Lipman, D. J. *J. Mol. Biol.* **1990**, *215*, 403.